24th ABCM International Congress of Mechanical Engineering
December 3-8, 2017, Curitiba, PR, Brazil

COBEM-2017-0342
EFFECTS OF PRIOR HEAT TREATMENT ON AISI 420 STEEL LOW-TEMPERATURE PLASMA NITROCARBURIZING

Cristiano José Scheuer
Industrial Technical College, *Universidade Federal de Santa Maria, Santa Maria-RS, 97105-900, Brazil.*
e-mail: cristiano.scheuer@smail.ufsm.br

Adriano David dos Anjos
Instituto Federal do Paraná, Campo Largo-PR, 87360-000, Brazil.
e-mail: adriano.anjos@ifpr.edu.br

Rodrigo Perito Cardoso
Plasma Assisted Manufacturing Technology and Powder Metallurgy Group, *Universidade Federal do Paraná, Curitiba-PR, 81531-980, Brazil.*
e-mail: rodrigo.perito@ufpr.br

Sílvio Francisco Brunatto
Plasma Assisted Manufacturing Technology and Powder Metallurgy Group, *Universidade Federal do Paraná, Curitiba-PR, 81531-980, Brazil.*
e-mail: brunatto@ufpr.br

Abstract. *Plasma surface treatments have been applied to a large extent on tools and industrial components to improve their surface properties. Several methods for plasma diffusion process, such nitriding, carburizing, nitrocarburizing, etc., have been developed as primary surface hardening process. Nitrocarburizing is one of the most applied methods for improving mechanical and corrosion resistance of engineering materials. It involves the nitrogen and carbon introduction into the component surface, to produce a compound layer with mixed* ε*-Fe2-3(N,C) phases and a interstitial solid solution of nitrogen and carbon. Such nitrocarburized generated phases are known to be valuable to the tribological properties due to the inherently high internal stresses arising in the lattice parameter. However, on stainless steels treatment, chromium carbides/nitrides precipitation can occur when treatments were carried out at high temperature or for excessive time, resulting in a depletion of stainless steel corrosion resistance. For martensitic stainless steels, special attention should be credited on choice of heat pretreatment conditions, once materials microstructure and defect density, resulting of heat treatment, affect the carbon and nitrogen diffusion kinetics. Thus, this research aims to investigate the effect of heat pretreatment in growth kinetics and mechanical properties of nitrocarburized layer produced on AISI 420 steel. Thereunto, plasma nitrocarburizing treatments were carried out using DC-pulsed power supply in a 71%* N_2 *+ 18%* H_2 *+ 10% Ar + 1%* CH_4 *gas mixture, at temperatures of 300 to 450 °C, and times of 2 to 12 h for annealed, as-quenched and tempered AISI 420 steel. The applied peak voltage, gas flow rate and pressure were kept constant at 600 V,* 3.32×10^{-6} *Nm*^{3} *s*$^{-1}$ *and 400 Pa, respectively. The treated samples were characterized by optical microscopy, X-ray diffractometry and microhardness measurements. Results demonstrate that the nitrocarburized layer growth kinetics depends on the samples prior heat treatment. Plotting layer thickness data on an Arrhenius plot, two slopes can be observed, indicating different activation energies for high and low temperatures treatments. Finality, XRD data show that chromium nitride/carbide precipitation occurs for temperatures above 400 °C, as illustrated by the micrographs.*

Keywords: *martensitic stainless steel, low temperature plasma nitrocarburizing, expanded martensite, prior heat treatment, process kinetics.*

1. INTRODUCTION

Surface properties of AISI 420 martensitic stainless steel can be achieved through plasma assisted carburizing (Scheuer et al. 2012) or nitriding treatments (Leyland et al. 1993) application, due to the very high near surface concentrations of interstitially dissolved carbon or nitrogen atoms. In these treatments, chromium carbide and nitride formation is inhibited kinetically, since the low processing temperatures effectively immobilize the substitutional elements, and a supersaturation of interstitially dissolved carbon or nitrogen is achieved. Therefore, an increase in the mechanical and tribological properties is obtained without damage to the corrosion resistance (Angelini et al. 2016, Scheuer et al. 2016, Xi et al. 2008). Treatments that combine difusion simultaneous of both carbon and nitrogen, denoted as nitrocarburizing, can also be applied for surface hardness increasing of the AISI 420 steel (Anjos et al. 2015). Considering that martensitic stainless steels are metastable Fe alloy, special attention must be credited to previous heat treatment conditions selection. These treatments have important effects on low-temperature plasma thermochemical processes, since they cause important variations in the steel microstructure and defect density, reflecting directly in the treated layer growth and secondary phases precipitation kinetics (Cardoso et al. 2016). Considering that low-temperature plasma assisted treatments presents low kinetics, which is not des irable from the economical purposes, different studies have been developed aiming to enhance the treatment kinetics by enhancing the high diffusivity paths contribution, like grain boundaries and dislocations (considering that the diffusion by such paths has activation energy that is significantly lower than the volume diffusion, being easily activated at low temperature) (Cardoso et al. 2016). On martensitic stainless steels, this kinetics enhancement can be obtained mainly by changing the prior heat treatment, by means of increasing the defect density. Thus, this work had as purpose to study the effect of the prior heat treatment effect on nitrocarburized layer growth and secondary phase precipitation kinetics, in AISI 420 martensitic stainless steel.

2. EXPERIMENTAL PROCEDURE

Cylindrical samples of 10 mm in height and 9.5 mm in diameter were cut from AISI 420 martensitic stainless steel commercial bar. Annealed samples were obtained just cutting the rod. To obtain the as-quenched samples, they were austenitized at 1050 °C for 0.5 h and air cooled; and, to obtain the tempered samples, as-quenched samples were tempered at 400 °C for 1 h. The sample hardness in the annealed, as-quenched and tempered conditions were 327±13, 510±11 and 420±17 $HV_{0.3}$. After heat treatment, samples were grounded and mirror polished, to obtain a standard surface initial condition, using SiC sandpaper ranging from 100 to 1200 grade and 1 μm Al_2O_3 abrasive suspension, respectively. Finally, samples were alcohol cleaned in ultrasonic bath and then introduced into the discharge chamber.

Aiming to remove the native oxide layer from sample surface, before nitrocarburizing, specimens were plasma sputter-cleaned in a gas mixture of 80% H_2 + 20% Ar, under a pressure of 400 Pa, at 300°C for 0.5 h. Plasma nitrocarburizing was carried out using a gas mixture composed of 71% N_2 + 18% H_2 + 10% Ar + 1% CH_4, in volume. The total gas flow rate and pressure were fixed at 3.34×10^{-6} $Nm^3 s^{-1}$and 400 Pa, respectively. Samples were nitrocarburized at 300, 350, 400 and 450ºC, for 2, 4, 6 and 12 h. The plasma apparatus, illustrated and presented in detail by Scheuer et al. (2013), consisted of a 4.16 kHz square-wave pulsed DC power supply and a stainless steel cylindrical vacuum chamber of 350 mm in diameter and 380 mm high, attached to steel plates sealed with silicone o-rings at both the ends. The system was pumped down to a residual pressure on the order of 3 Pa using a double stage mechanical vacuum pump. The gas flow rate and composition was adjusted by using four mass flow controllers, three of 8.33×10^{-6} $Nm^3 s^{-1}$, for H_2, Ar and N_2, and one of 8.33×10^{-8} $Nm^3 s^{-1}$, for CH_4.

Annealed, as-quenched and tempered samples were placed on the cathode of the discharge (employing a samples holder similar to that used by Cardoso et al. (2016), which was negatively biased at 600 V. The heating of the samples was a result of ions and fast neutrals species bombardment. The mean power transferred to the plasma, and consequently the treatment temperature, was adjusted by varying the switched-on time (t_{ON}) of the pulsed voltage. The temperature was measured by means of a chromel-alumel thermocouple (K–type of 1.5 mm diameter) inserted 8 mm depth into the sample holder. The pressure in the vacuum chamber was measured by a capacitive manometer of 1.33×10^4 Pa in full-scale operation and adjusted by a manual valve.

For microstructural analysis, samples were prepared by conventional metallographic procedure. After polishing, the cross-sectioned samples were etched using Vilella's reagent (95 ml of ethyl alcohol, 5 ml of hydrochloric acid, and 1 g of picric acid). Samples were examined using an Optical Microscope (Olympus BX51M). The identification of the phases present in the treated layers was carried out by X-ray diffractometry (XRD), using a Shimadzu XDR 7000 X-ray diffractometer with a CuK_α X-ray tube in the Bragg-Brentano configuration. Hardness measurement were performed by using a Shimadzu Micro Hardness Tester HMV2T, applying a load of 300 gf and a peak-load contact of 15 s. The indicated values in the hardness profiles correspond to the mean of five measurements.

3. RESULTS AND DISCUSSION

The cross-section micrograph of as-quenched, tempered and annealed samples plasma nitrocarburized at 300 to 450 °C for 6 h are presented in Figure 1. For low-temperature treated samples (equal or below to 350 °C), the chemically altered surface (treated layer) is not affected by the etchant. In this case, no sharp interface between the treated layer and the substrate bulk is noted. For higher nitrocarburizing temperatures (from 400°C), the interface can be easier defined. Since the etchant do not attack the chemically-altered surface region while the unaltered bulk is being etched, it is clear that the obtained nitrocarburized layer, at low temperatures, tends to present an increased etching resistance to Vilella's reagent when compared to the AISI 420 MSS substrate, being an indication of improved corrosion resistance. In contrast, for high temperature treated samples (equal or above 400 °C), dark-aspect regions are noticed in the nitrocarburized layers, indicating the treated surface sensitization, which is due to chromium nitride/carbide precipitation (as confirmed by the XRD patterns showed and discussed in the sequence) and consequent reduction of the chromium content in solid solution. Likewise, for the high temperature treatment conditions, two different treated regions can be distinguished from the top surface to the substrate bulk, in the case, a dark-aspect layer near the surface precipitation zone followed by a white aspect layer, probably free of chromium carbide/nitride precipitation, defining the interface between the treated surface and the substrate bulk. It can also be noted, by comparing the microstructural differences of the samples with different prior heat treatment, that the as-quenched samples are less subjected to sensitization for a given nitrocarburizing temperature when compared to tempered and annealed ones. This dissimilarity can be attributed to differences in chromium content in solid solution or defect density promoting carbon and nitrogen diffusion. For the case of tempered samples, the diffusion of Cr during tempering results in fluctuations of composition all over the steel matrix, leading to Cr enriched regions to be formed, favoring carbide and nitride precipitation during the nitrocarburizing process.

X-ray diffraction patterns of as-quenched, tempered and annealed samples nitrocarburized at 300 to 450 °C for 6 h are presented in Figure 2. The untreated sample presents one major peak attributed to the martensite phase (α'). According to the treatment temperature, changes in the constituents of the nitrocarburized layer can be observed through the obtained XRD patterns. It is worth to be reported the Fe_3C, $Fe_{2-3}N$ and α'_{NC} (expanded martensite) phases formation for low-temperatures nitrocarburized (less than 350 °C). As already widely discussed in the literature, the expanded martensite phase formation is evidenced by the original martensite peaks broadening and displacement to lower angles. For high-temperature nitrocarburizing (from 400 °C), peaks of CrN and $Cr_{23}C_6$ are also observed, confirming the sensitization observed in Figure 1. It can also be noticed that the expanded martensite peaks disappear for samples treated at 450 °C, indicating that the α'_{NC} phase decomposes at the expense of intense nitride formation, which leads the carbon and nitrogen amount initially present in the expanded martensite phase to decrease, giving rise to XRD patterns constituted only by nitride phases. From the Figure 1 (b) and (c) it can be observed that the as-quenched samples presented more intense peaks of α'_{NC} phase, comparing with that observed for tempered and annealed samples. This result can be attributed to the higher solid solution chromium content and, theoretically, a more homogenous chromium distribution all over the matrix, leading to a higher nitrogen/carbon solubility/super-saturation in the martensite lattice in the case of the as-quenched samples.

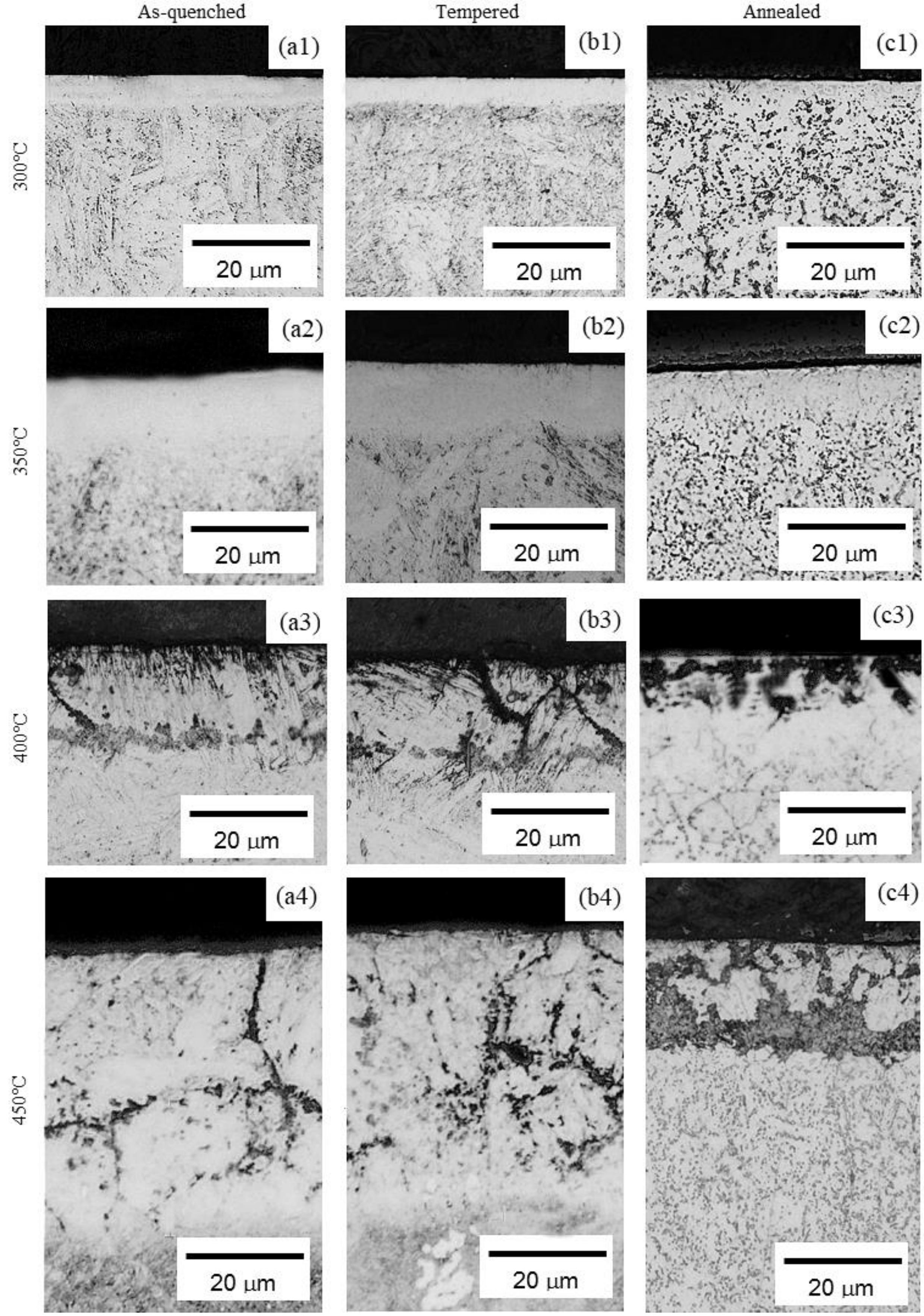

Figure 1. Cross-section micrographs of (a) as-quenched, (b) tempered and (c) annealed samples nitrocarburized at (1) 300°C, (2) 350°C, (3) 400°C and (4) 450 °C for 6 h.

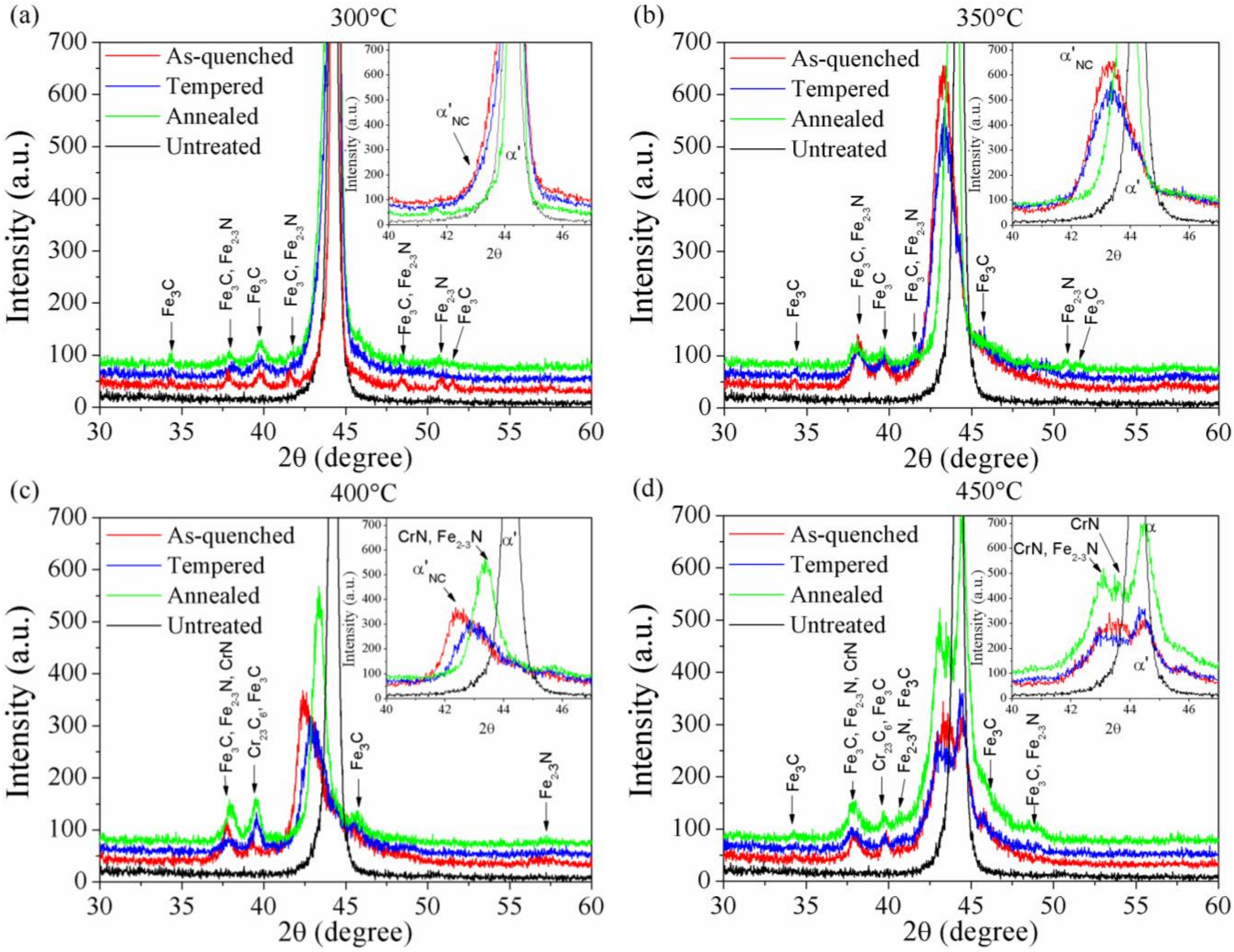

Figure 2. X-ray diffraction patterns for untreated and as-quenched, tempered and annealed samples nitrocarburized samples treated at (a) 300, (b) 350, (c) 400 and (d) 450 °C for 6 h.

Figure *3* presents the Arrhenius plot of the nitrocarburizing layer thickness for annealed, tempered and as-quenched samples treated at (a) 2, (b) 4, (c) 6 and (d) 12 h. The activation energy for nitrogen diffusion can be obtained assuming that the limiting process for the nitrocarburizing layer growth is the interstitial elements diffusion and that the layer thickness is proportional to the square root of the nitrocarburizing time. In this case, the activation energy for interstitial elements diffusion during the nitrocarburizing process can be obtained by the slope of the ln (d) x 1/T plot. From the Arrhenius plot, it becomes evident that at high temperatures, in this case higher than 400 °C, the limiting process for the layer growth tends to have the same activation energy. This could be expected since the diffusion/nitrocarburizing process tends to the equilibrium and the volume diffusion is expected to be the main diffusion process for all kind of prior heat treatment. Moreover, the activation energy for annealed samples do not change in the whole studied temperature range, since annealed samples are in equilibrium state and high diffusivity paths are expected to be negligible in the referred range. Finally, and more important, at low temperatures the activation energy is lower for as-quenched and tempered samples when compared with the annealed samples. This results can be attributed to the defect density or to the influence of chromium content in solid solution, making evident the contribution of the high diffusivity paths for low-temperature nitrocarburizing process.

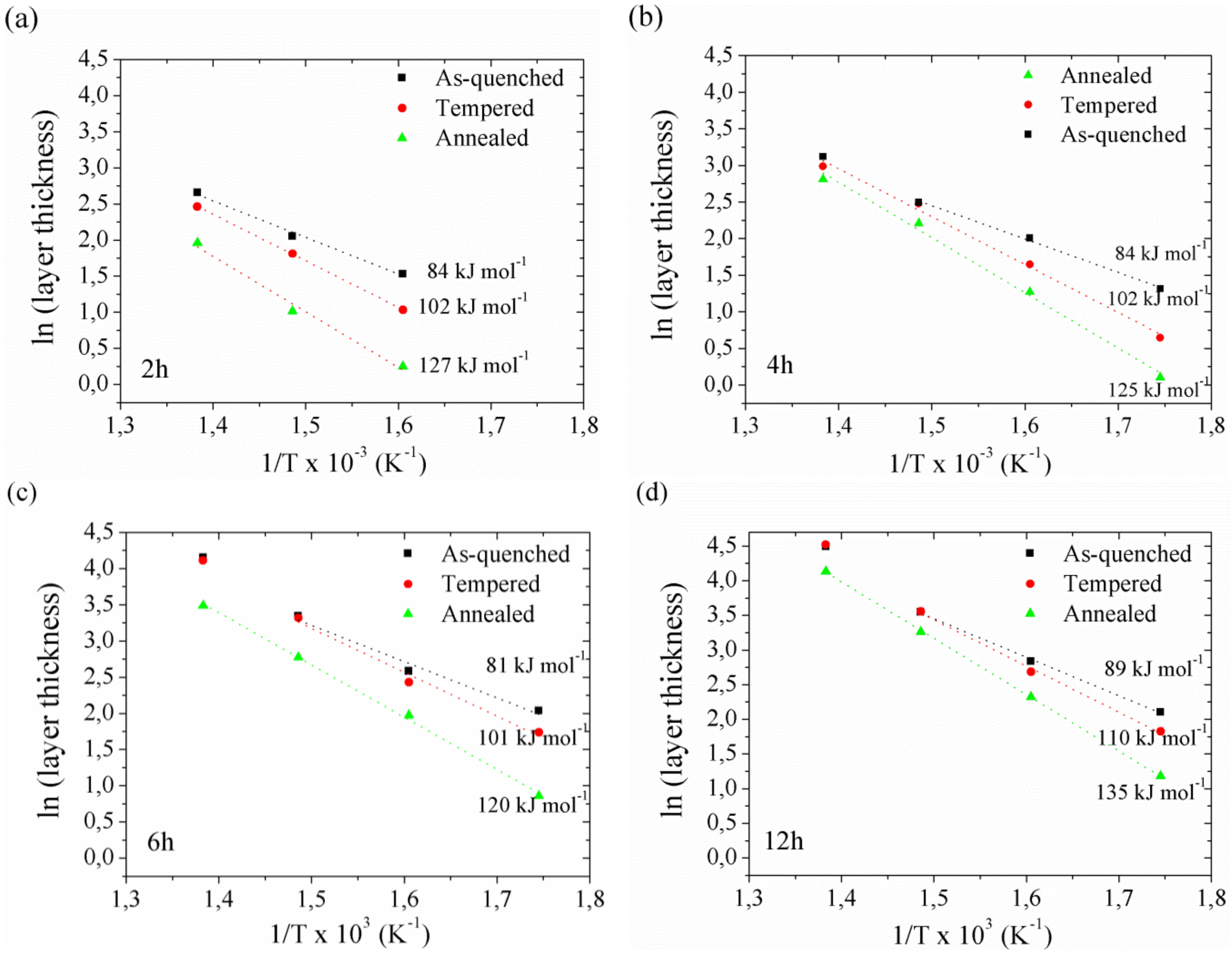

Figure 3. Arrhenius plot for the as-quenched, tempered and annealed samples nitrocarburized at: (a) 2 h, (b) 4 h, (c) 6 h, and (d) 12 h.

The evolution of the nitrocarburizing layer thickness as a function of the square root of treatment time is presented in Figure 4 for (a) as-quenched, (b) tempered and (c) annealed samples. Extrapolating the curves, considering that the nitrocarburizing layer growth is proportional to the square root of treatment time, two results can be observed: i) the low-temperature plasma nitrocarburizing presents an incubation time for the layer formation; and ii) the incubation time is higher for higher treatment temperatures. In this case, incubation time was assumed to be the time necessary to remove the passive oxide layer from the surface of samples, enabling the interstitial elements diffusing into the substrate. The longer incubation time for nitrocarburzing layer growth at high temperatures is linked to defects annihilation and grain growth occurred at sufficiently high temperatures treatment conditions, reducing the layer growth kinetics. Finally, it seems that the prior heat treatment do not play an important role on the layer thickness time behaviour for the studied conditions.

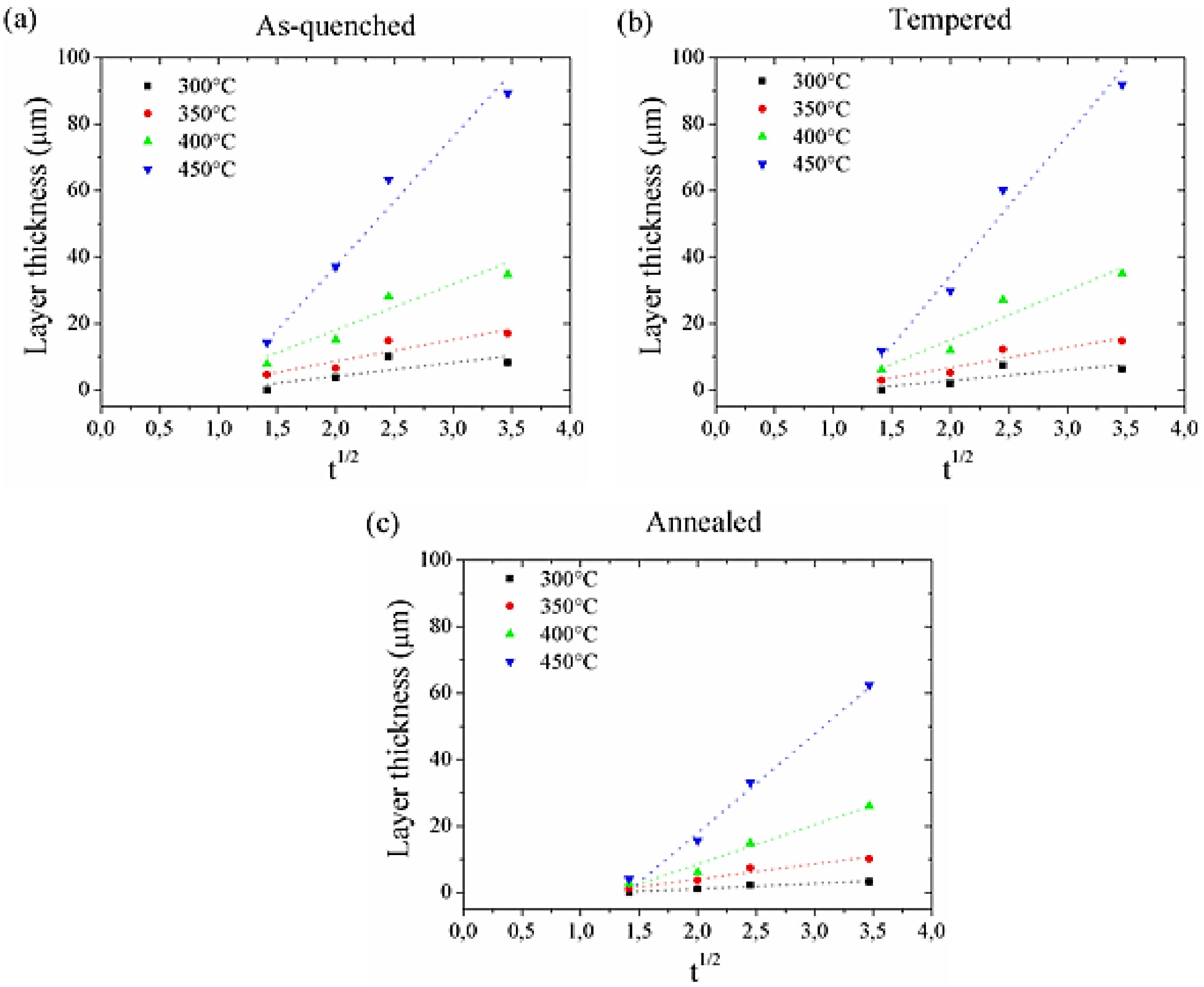

Figure 4. Nitrided layer thickness as a function of the square root of nitriding time for (a) as-quenched, (b) tempered and (c) annealed samples.

Figure 5 depicts the cross section micrographs of as-quenched samples treated at (a) 2, (b) 4, (c) 6 and (d) 12 h for (1) 300, (2) 350, (3) 400 and (4) 450 °C. It can be observed that an incipient sensitization along the grain boundaries close to the surface is observed for samples nitrocarburized for 2 h at 400 °C, evidencing that Cr carbide/nitride precipitation starts at this temperature for 2 h treatment time. The sensitization is intensified with the increase in treatment time to 6 h, and at 12 h the it is generalized all over the nitrocarburized layer. For this last condition, the sensitization occurs already for the sample treated at 350 °C. It clearly illustrates how the treatment time can be important for low-temperature nitrocarburizing of stainless steels.

The evolution of surface hardness of as-quenched, tempered and annealed samples plasma carburized from 300 to 450 °C at 2 to 12 h is presented in Figure 6. The hardness grows with the increase in treatment temperature and time. This growth can be due to the actual hardness of the treated layer and also to the treated layer thickness, which can be of the same order of magnitude of the indentation depths. It is found that, for most conditions, the surface hardness is higher for as-quenched samples when compared to the other conditions, which can be attributed both to the higher growth kinetics and to the higher amount of α'_{NC} phase. The decrease in hardness values for high temperatures treatment is due the chromium carbinde/nitride precipitation, leading the α'_{NC} amount to be diminished, resulting in surface hardness decrease. This result indicate that the prior heat treatment has significant influence on the mechanical properties of the treated surface and that α'_{NC} phase has important hardening effect in low-temperature nitrocarburizing of martensitic stainless steels. For temperatures higher than those presented in Figure 6 it is expected that the surface hardness of all type of samples will tend to the same value, since both iron and chromium carbide/nitride formation become the most important surface hardening mechanism.

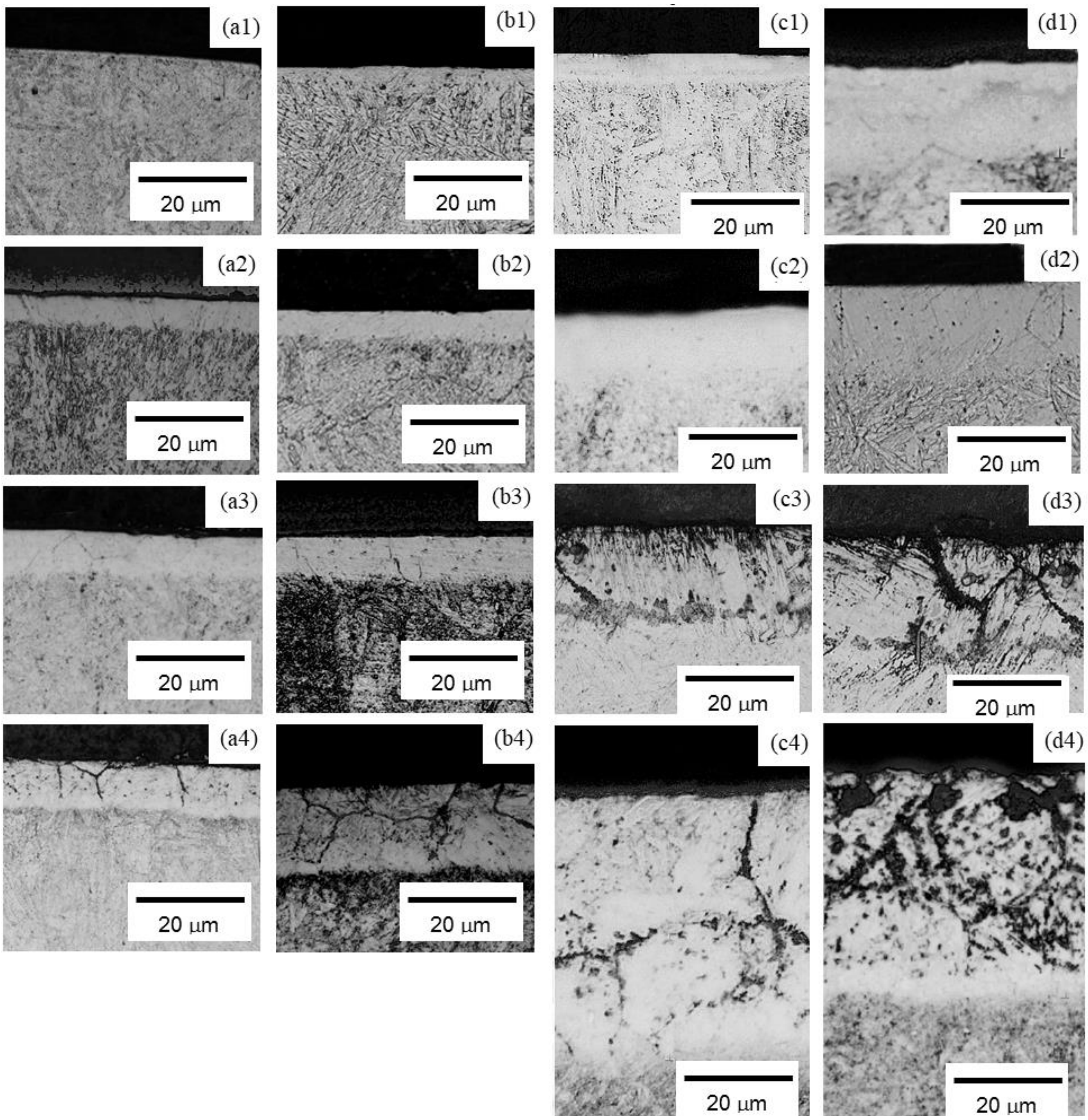

Figure 5. Cross-section micrographs of as-quenched samples nitrocarburized for (a) 2, (b) 4, (c) 6 and (d) 12 h at (1) 300, (2) 350, (3) 400 and (4) 450 °C.

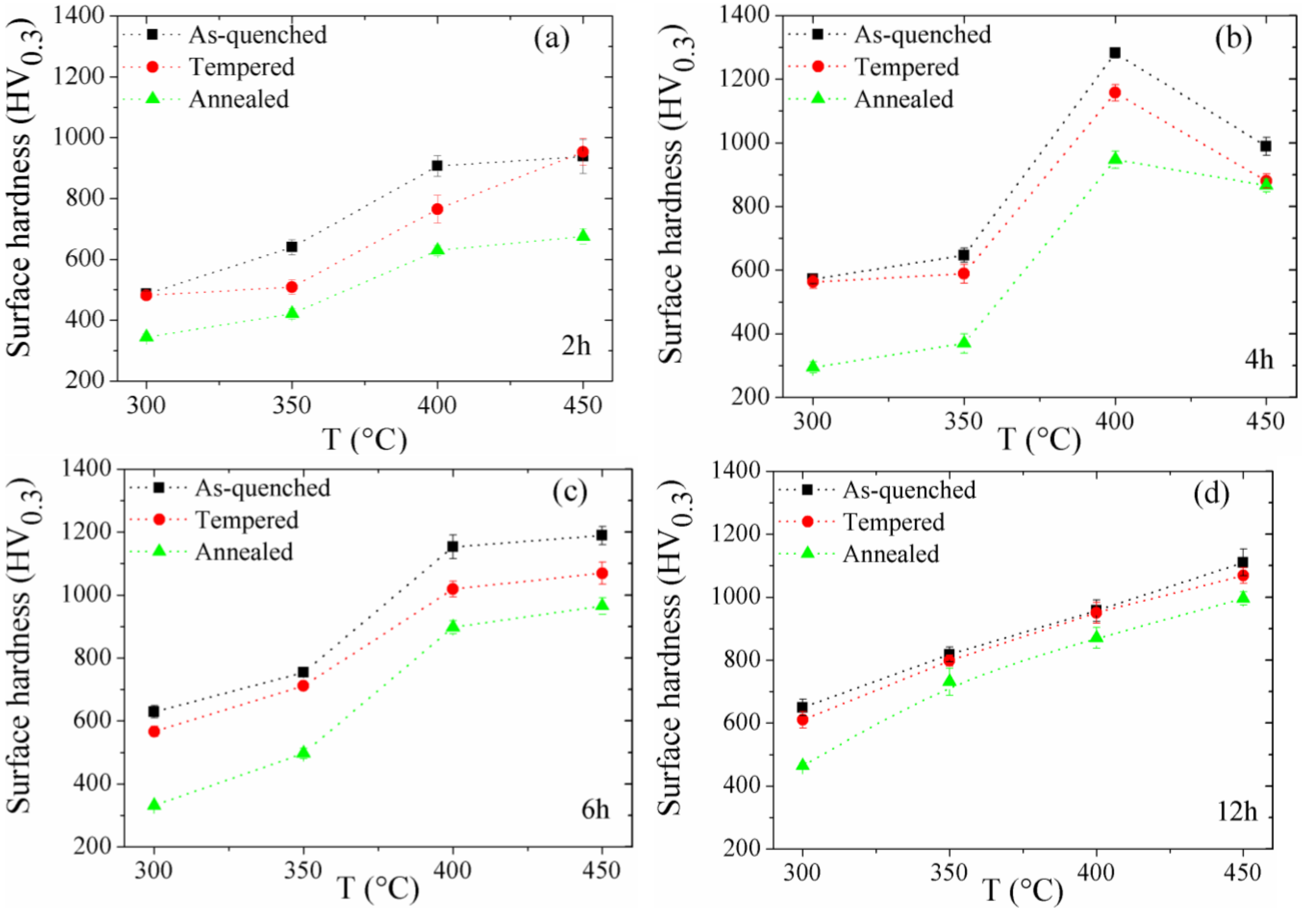

Figure 6. Hardness of as-quenched, tempered and annealed samples nitrocarburized at 300 °C, 350 °C, 400 °C, 450 °C and 500 °C for: (a) 2 h, (b) 4 h, (c) 6 h, and (d) 12 h.

4. CONCLUSION

A comprehensive study was carried out aiming to illustrate the influence of prior heat treatment on the low-temperature nitrocarburizing process, focusing on the process kinetics and mechanical properties of the treated layer. AISI 420 martensitic stainless steel samples prepared in three different prior heat treatment conditions were low-temperature plasma nitrocarburized. The main conclusions of the research can be listed as follows:

- At sufficient low temperatures and times, a precipitation-free nitrided layer is produced. On the other hand, at high temperature and time, the chromium mobility promotes $Cr_{23}C_6$ and CrN precipitation, reducing the chromium content in solid solution and causing a reduction in the material corrosion resistance (sensitization). Moreover, precipitation of carbides/nitrides also reduces the carbon/nitrogen content retained in solid solution and the α'_{NC} phase amount. It is accompanied by hardness reduction of the nitrocarburized surface;
- The prior heat treatment has remarkable influence on the low-temperature nitrocarburizing of martensitic stainless steels. Starting from the same base material, nitrocarburizing process kinetics and mechanical properties of the treated surfaces can considerably change if different prior heat treatment is applied;
- Finally, at high temperatures the layer growth tends to have the same activation energy for all studied previous heat treatment, probably related to volume diffusion of interstitial elements dominating the process. However, at low temperatures, the activation energy is lower for as-quenched and tempered samples when compared with annealed samples. It can be attributed to the defect density or to the influence of chromium content in solid solution, related to high diffusivity paths diffusion contribution to the interstitial elements diffusion into the substrate.

5. REFERENCES

Angelini, V.; Boromei, I.; Martini, C.; Scheuer, C.J.; Cardoso, R.P.; Brunatto, S.F.; Ceschini, L. Dry sliding behavior (block-on-ring tests) of AISI 420 martensitic stainless steel, surface hardened by low temperature plasma-assisted carburizing. *Tribology International* 103 (2016) 555–565.

Anjos, A.D.; Scheuer, C.J.; Brunatto, S.F.; Cardoso, R.P. Low-temperature plasma nitrocarburizing of the AISI 420 martensitic stainless steel: Microstructure and process kinetics. *Surface and Coatings Technology* 275 (2015) 51–57.

Cardoso, R.P.; Scheuer, C.J.; Brunatto, S.F. Low-Temperature Nitriding Kinetics of Stainless Steel: Effect of Prior Heat Treatment. *Encyclopedia of Iron, Steel, and Their Alloys*. 1ed.: Taylor & Francis Group 2 (2016) 2153–2168.

Leyland, A.; Lewis, D.B.; Stevenson, P.R.; Matthews, A. Low temperature plasma diffusion treatment of stainless steels for improved wear resistance. *Surface and Coatings Technology* 62 (1993) 608–617.

Scheuer, C.J.; Cardoso, R.P.; Mafra, M.; Brunatto, S.F., AISI 420 martensitic stainless steel low-temperature plasma assisted carburizing kinetics. *Surface and Coatings Technology*. 214 (2013) 30– 37.

Scheuer, C.J.; Cardoso, R.P.; Pereira, R.; Mafra M.; Brunatto, S.F. Low temperature plasma carburizing of martensitic stainless steel. *Materials Science and Engineering*: A 539 (2012) 369–372.

Scheuer, C.J.; Cardoso, R.P.; Possoli, F.; Borges, P.C.; Brunatto, S.F. Corrosion behavior of low-temperature plasma carburized AISI 420 steel - part I - effect of treatment temperature. In: I*X Congresso Nacional de Engenharia Mecânica*, 2016.

Xi, Y.; Liu, D.; Han, D. Improvement of corrosion and wear resistances of AISI 420 martensitic stainless steel using plasma nitriding at low temperature. *Surface and Coatings Technology* 202 (2008) 2577–2583.

6. RESPONSIBILITY NOTICE

The authors are the only responsible for the printed material included in this paper.